WiFED: WiFi Friendly Energy Delivery with Distributed Beamforming

Subhramoy Mohanti*, Elif Bozkaya†‡, M. Yousof Naderi*, Berk Canberk† and Kaushik Chowdhury*

*Department of Electrical and Computer Engineering, Northeastern University, Boston, USA
†Department of Computer Engineering, Istanbul Technical University, Istanbul, Turkey
‡Department of Computer Engineering, National Defense University Naval Academy, Istanbul, Turkey
Email: smohanti@coe.neu.edu, bozkayae@itu.edu.tr, naderi@coe.neu.edu, canberk@itu.edu.tr, krc@ece.neu.edu

Abstract—Wireless RF energy transfer for indoor sensors is an emerging paradigm that ensures continuous operation without battery limitations. However, high power radiation within the ISM band interferes with the packet reception for existing WiFi devices. The paper proposes the first effort in merging the RF energy transfer functions within a standards compliant 802.11 protocol to realize practical and WiFi-friendly Energy Delivery (WiFED). The WiFED architecture is composed of a centralized controller that coordinates the actions of multiple distributed energy transmitters (ETs), and a number of deployed sensors that periodically request energy from the ETs. The paper first describes the specific 802.11 supported protocol features that can be exploited by WiFED for sensors to request energy and for the ETs to participate in the energy delivery process. Second, it devises a controller-driven bipartite matching-based algorithmic solution that assigns the appropriate number of ETs to specific energy requesting sensors, resulting in a highly efficient energy transfer process. The proposed in-band and protocol supported coexistence in WiFED is validated via simulations and partly in a software defined radio testbed, showing 15% improvement in network lifetime and 31% reduction in the charging delay compared to the classical nearest distance-based charging schemes that do not anticipate future energy needs of the sensors and which are not designed to co-exist with WiFi systems.

I. Introduction

The pervasive deployment of heterogeneous sensors and small form-factor computing devices in homes and manufacturing floors is already showing tremendous gains in user-convenience, operational efficiency in terms of time and energy, and enhanced safety [1]. However, by design, these sensors are typically low-cost devices with limited energy storage capacity. Contact-less wireless energy transfer is a promising technique that overcomes physical battery replacements and ensures continued, reliable operation. One such approach is based on focused RF radiation from energy-rich sources, which can then be stored at the sensors for future use. However, several challenges must be addressed to realize this vision, specifically in terms of coexistence with other legacy wireless devices communicating in the ISM bands and the achievable energy yields to make the system practicable. Our proposed approach called WiFi Friendly Energy Delivery (WiFED) addresses both these concerns by coexisting with and leveraging the 802.11 standard, as well as performing digital beamforming with the help of multiple different energy transmitters (ETs).
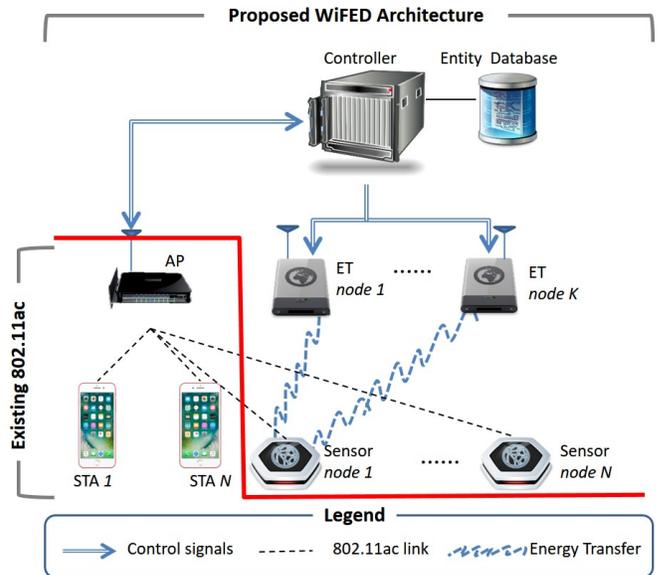

Fig. 1. WiFED architecture for energy delivery with distributed beamforming over existing 802.11ac network.

WiFED operates in the presence of a regular 802.11 WiFi access point (AP) with its associated clients stations (STAs). Our work is applicable to forward looking WiFi standards, including 802.11ac and beyond, which incorporates advanced features at the MAC layer that we will describe later in the paper. For concrete implementation example and without loss of generality, we shall directly reference 802.11ac standard in the subsequent discussion. WiFED introduces to an existing WiFi network, few key components given in Figure 1: (1) deployed IoT sensors that have a compatible 802.11ac WiFi radio and interfaced with an RF harvesting circuit; (2) multiple distributed ETs, each consisting of a radio with two operational modes: one that supports 802.11ac and the second mode that transmits an unmodulated continuous wave signal with maximum possible power ($\leq 3W$ as per FCC rules) [2]; and (3) a controller that coordinates the energy transfer process, which can either exist as a separate device or be embedded as a software entity within the AP.

A. WiFED Motivation and Novelty

Existing 802.11-family of protocols are not designed for coexistence with heterogeneous networks. Thus, even if highly

1

efficient RF energy transfer is achieved, it is difficult to implement this in practical co-channel home/factory environments. Several IoT applications may provide critical services that require the sensor to be always operational. In such cases, the energy transfer takes priority. WiFED leverages existing 802.11ac protocol features to provide this differentiated channel access priority between energy and data transfers. Solutions such as a specialized MAC [3]-[4] or modulating the energy signal with data [5] require changing existing WiFi infrastructure and rely on non-standardized protocols. WiFED is designed ground-up to facilitate both compatibility and coexistence with the 802.11ac (and later) standards; it can be deployed with current off-the-shelf hardware. Finally, WiFED addresses a fundamental problem in indoor deployments of selecting an optimal subset of ETs for each incoming energy request from a target sensor.

B. Conceptual Overview of WiFED Operation

WiFED builds on top of the existing 802.11ac WiFi architecture by innovatively introducing an energy plane along with the existing data and control planes. Here, the 802.11ac compatible AP manages all STA nodes (sensors and other users) in its Basic Service Set (BSS). The energy requests originate from individual sensors and are transmitted in the form of regular data packets towards the centralized controller, via the AP. The controller keeps a database of all registered sensors and ETs. The controller now identifies the optimal subset of sensors, via a bipartite matching algorithm, to create and assign groups of ETs to requesting sensors. It then instructs the AP to set up a contention-free period (CFP) for the energy transmission as well as initializes the ETs for the upcoming energy transfer, specifying the duration for which the target sensors should be charged. The energy transfer duration is upper bounded to ensure that data communication occurs fairly within the same channel.

The rest of the paper is organized as follows: Sec. II describes the related works and Sec. III presents the preliminary experiments that justify and motivate the WiFED design. In Sec. IV, we explain the details of WiFED system operation. The WiFED energy scheduling framework is explained in detail in Sec.V. We perform extensive performance evaluation studies in Sec.VI. Finally, Sec.VII concludes the paper.

II. RELATED WORK

In this section, we review the most relevant works in three areas as follows.

Wireless Charging Protocols and Platforms: Protocols and platforms for RF energy transfer and harvesting have been comprehensively surveyed recently in [6]-[7]. MAC protocols that investigate the impact of sensor placement, frequency of operation, and number of RF energy transmitters on wireless charging time for optimizing energy delivery while minimizing its effect on data communication have been proposed in [3]-[4]. However, a clean-state MAC design is difficult to implement without costly integration overheads.

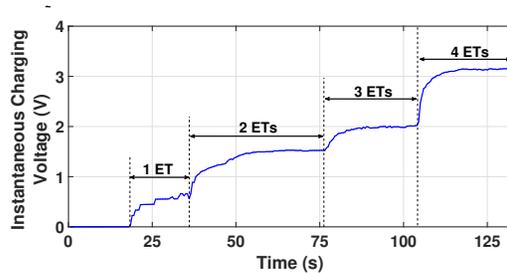Self-sustainable wireless nodes by harvesting ambient RF energy in specialized cognitive radio networks is proposed

Fig. 2. Instantenous charging voltage at receiver with 1, 2, 3 and 4 ETs beamforming sequentially.

in [8], where low power secondary nodes harvest energy from nearby high power primary nodes. However, realistic power levels for such an architecture are not possible for indoor scenarios, as apart from requiring dedicated spectrum. Other works include harvesting energy from the received signals using time switching and power splitting methods while minimizing the impact on data performance [9]. All these works, while furthering the state-of-the-art, do not focus on WiFi coexistence, and require considerable engineering of the protocol stack. The problem of multiple device charging by a limited set of energy transmitters has been considered in [10]. WiFED also incorporates this approach but under realistic characteristics of RF energy harvesting circuits.

Energy Transfer and Data Co-existence: Co-channel data and energy transfer is proposed in [5] by introducing a novel physical layer modulation scheme where the sender introduces variations in the envelope of the energy signal to communicate data. This scheme requires complex synchronization with existing upper layers of network and available hardwares. The authors in [11] study the effect of ET placement on the charging rate of the sensor nodes and impacts on data communication, quantitatively analyzing the tradeoffs between wireless energy harvesting and data transfer.

III. EXPERIMENTS ON DISTRIBUTED BEAMFORMING

In this section we describe the preliminary experiments carried out to evaluate the distributed beamforming and coexistence mechanisms in order to benefit both energy and data transfer processes in the 2.4GHz ISM band. Specifically, we observe interference and performance characteristics between 802.11ac data and energy transmission with (i) continuous energy beamforming, (ii) random energy beamforming, and (iii) WiFED framework.

• **Distributed Energy Beamforming Experiments**: In the first step, we demonstrate the feasibility of a distributed energy transfer network that uses beamforming through real testbed [12], where multiple ETs are synchronized in phase and frequency in real time using periodic feedback from the target sensor, but without any common clock reference. Our beamforming setup consists of the following components 1) Four programmable ETs with omnidirectional antennas, 2) one RF-energy harvester circuit, and 3) controller software. A programmable ET is basically a Universal Software Radio Peripheral (USRP) connected to a power amplifier. The RF-energy harvester is fabricated and connected to a TI EZ430
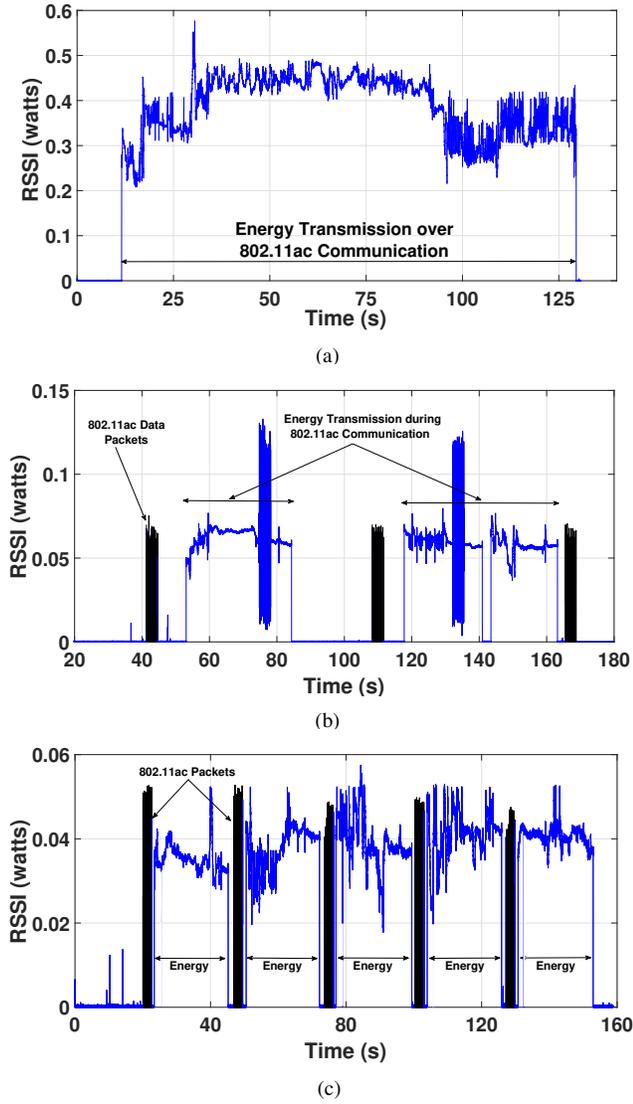
Fig. 3. Effect of energy transfer in different modes: (a) continuous energy transfer, (b) random energy transfer, (c) controlled energy transfer.

sensor. The GNURadio software plane in the USRPs implements the beamforming algorithm for phase and frequency synchronizations, and transfers high power energy signals toward the desired receiver using a power amplifier with maximum allowable power. Using distributed energy beamforming, ETs self-adjust their in-phase based on feedback from the receiver, so that maximum net energy is transferred towards the intended receiver. The ETs organize themselves into a virtual antenna array and focus their transmission energy in the direction of the sensor, such that the emitted waveforms add up constructively at the target sensor. If all radios have the same antenna gain G_t and transmission powers P_t, with the receiver gain be G_r, then the received power P_t^r at the receiver node simplifies to:

$$P_T^r = P_t G_t G_r (\frac{\lambda}{4\pi})^2 \Big[\sum_{i=1}^{N} \frac{1}{R_i^2} + \sum_{i=1,i\neq j}^{N} \sum_{j=1}^{N} \frac{\cos(k\Delta R_{ij})}{R_i R_j} \Big]$$

(1)

where $k = 2\pi/\lambda$ is the wave number of the energy wave

(i.e., magnitude of the energy wave vector), $R_i = [(x_r - x_i)^2 + (y_r - y_i)^2]^{1/2}$ is the Euclidean distance from radio i to receiver and $\Delta R_{ij} = R(i) - R(j)$ is the difference between distances of radio i and j from the receiver. This analytical model for received power can be used to find the charging efficiency from N energy transmitting radios to each sensor. In our first set of energy beamforming experiments, four ETs are placed 20cm away from each other in an array, each connected to two 50Ω omnidirectional antennas. The distance from the transmitters and receiver are fixed at 1m. The ETs are successively turned on to perform beamforming and with all ETs having equal transmit power of 3W, we measured the different levels of energy at the receiver. From Figure 2, we see that the harvested voltage at the receiver increases exponentially with the increase in the number of ETs. Our experiment validates the analytical equation 1 and demonstrates the ability to efficiently transfer energy to sensors during their normal course of operations.

• **802.11ac and Energy Co-existence Experiments**: To characterize the effects of energy transmission in the ISM band of 2.4GHz during 802.11ac WiFi data communication, we created a 802.11ac WiFi AP and STA through Ettus USRP radios, and placed two ETs 1.5m apart from the WiFi link. MATLAB WLAN toolbox on the host machine was used to generate 802.11ac OFDM VHT packets which were transmitted using the connected USRP radio. On the receiver side, we used GNURadio companion to receive the data packets through the receiver USRP radio. For energy transfer, we used two other ETs tuned to the same 2.412 GHz with the host computer running the distributed beamforming algorithm. All of the host computers communicated with the controller via wired ethernet connections. The controller determined the duration and schedule of the energy beamforming to be either continuous, random or based on the WiFED framework. The WiFi transmission used 1 space-time stream of QPSK rate 1/2 configured to use a 160MHz bandwidth with the controller accurately scheduling transmission in the final scenario. We conducted the experiment with varying packet sizes of 1024, 1300, 1800 and 2000 bytes each time with 20 packets in a data slot and a total of 5 data slots.

• **Observations** We present our observations on concurrent energy and data transfer from the three modes of energy transfer through Figures 3 and 4 respectively. In Figure 3(a), we see that receiver only gets the energy signals at 0.4 Watts through continuous energy beamforming, while the data transmission gets completely interrupted by the higher power energy signal. As shown in Figure 4, throughput is negligible with 100% packet error rate (PER). In Figure 3(b) we observe the effects of signal reception when energy is transmitted at random intervals irrespective of data transmission. In this scenario, there is a high probability of data signals being interrupted by a random energy transfer. Though this is an improvement over the previous scenario of continuous energy transfer, this too adversely affects the data communication. As we can see from Figure 4 random interfering energy signal causes the WiFi receiver to attain almost half of the best achievable throughput
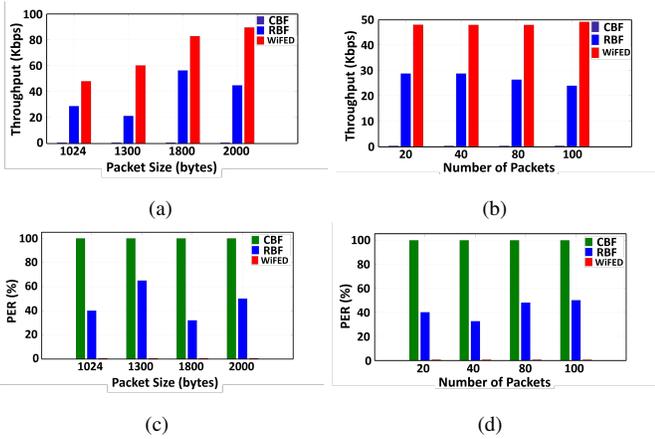
Fig. 4. Data performance characteristics of throughput with (a)changing packet size (b) number of packets. PER with (c) packet size and (d) number of packets in three modes of energy transfer.

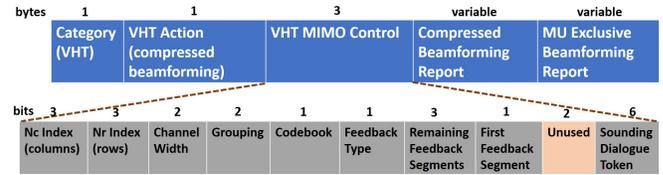| $UnusedFieldBits$	$EnergyRange(volts)$
00	1.8 - 2.25
01	2.26 - 2.7
10	2.71 - 3.15
11	3.16 - 3.6

Fig. 5. WiFED insertion of bit level sensor energy information in 802.11ac compressed beamforming action frame.

with around 40% PER. We compare these measurements with synchronized signal transmission scheduling shown in Figure 3(c). Here, we observe the controller synchronizes the energy transfer in between concurrent data transmission slots to avoid interference and enables co-existence with WiFi. We see that the throughput in Figure 4 achieves near-optimal rates in the absence of any interfering non-cooperating protocol, with negligible PER. Thus, we adopt this controller-driven synchronized approach in WiFED where the data communication is silenced through channel reservation using standards-defined 802.11ac protocol features.

IV. WiFED WITH 802.11AC-BASED CHANNEL ACCESS

WiFED operates the sensors in the Transmission Opportunity Power Save mode (TXOP PSM), as defined by the 802.11ac standard [13]. In this mode, the radio is kept switched off as a default case (called as Doze state), with periodic wakeup to check for currently buffered packets at the AP or to transmit new packets to the AP.

A. Managing Sleep-cycles Through 802.11ac

The pending packets at the AP for the sensors are informed via the Traffic Indication Map (TIM), transmitted in every beacon interval. Sensors wake up in the beacon transmission intervals to monitor downstream traffic. During a data transmission, sensors not involved in the ongoing transmission or reception consume a significant amount of energy in overhearing. To overcome this problem, TXOP PSM allows the sensor to sleep whenever it listens to a TXOP, in which the AP sends data to another STA. To do so, the AP indicates the duration of the ongoing TXOP in transmitted frames. Whenever an user receives a frame destined for another STA, a given sensor can switch to the sleep state and return to the awake state at the end of the TXOP. This operation, referred to as microsleep, lets the sensor sleep during short periods of time in which the channel is busy (typically, some tens, hundreds, or thousands of microseconds) [13].

B. Transmitting Energy Requests

Next, we describe how a sensor conveys its residual energy level to the controller through existing protocol fields defined by the 802.11ac standard. Specifically, we use the channel sounding function shown in Figure 6, which is periodically executed every 10ms-100ms by the AP, depending upon whether it is performing single-user or multi-user beamforming [14]. To achieve this, the AP sends out a Null Data Packet (NDP) after each NDP Announcement (NDPA) frame. Upon receiving the NDP, each associated STA in the network, including the sensors, reply back with the channel information in the Compressed Beamforming Action (CBA) frame. To query specific users, AP sends out the Beamforming Report Poll (BRP) for channel sounding measurement feedback following the NDP frame [15]. While the CBA frame is actually present to facilitate the AP-sensor communication (for data querying, sensing control directives etc.), WiFED piggybacks energy level information in the VHT MIMO Control field of CBA that has two unused bits, as shown in Figure 5. These two bits represent the four discrete energy states of the sensor as shown in the Table I, with $1.8V$ and $3.6V$ being the minimum and maximum operational energy limits. Note that these fields are populated only if there is a change from the previous reported energy level, else the bits remain unused. Additionally, we emphasize that sensors themselves do not participate in data/communication beamforming with the AP.

On receiving the CBA frame, the AP forwards the bit level information to the controller along with the Authentication ID (AID) of the sensor. From the energy levels from Table I, sensors reporting '00' will have the highest priority for their energy request; those reporting '11' will have the least priority. The controller translates the bit level information to the lowest voltage value in the corresponding energy range and proceeds to perform the energy monitoring, prediction, scheduling and sensor-ET mapping for beamforming, explained later in Section V.

C. Channel Reservation for Energy Transfer

The controller calculates the duration for the contention free period (CFP) based on the collective energy needs of the sensors, using the mathematical calculations in Sec. V. The AP then performs the following steps accordingly (see Figure 7):
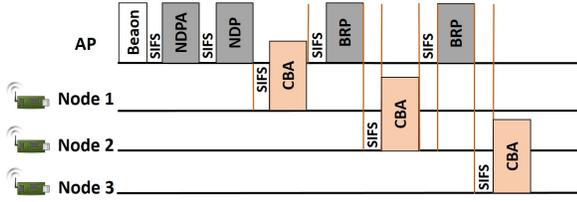
Fig. 6. WiFED sensor residual energy update through CBA frames during channel sounding procedure of 802.11ac protocol.
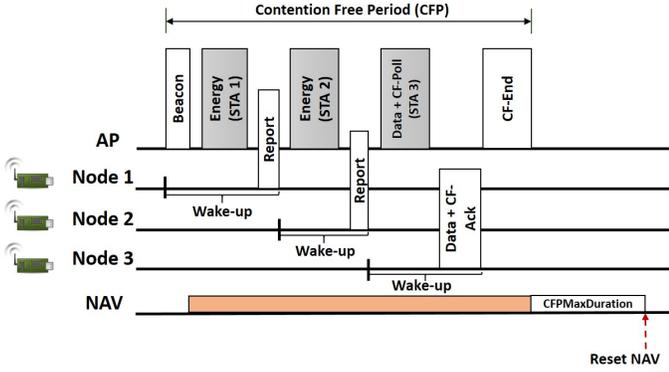

Fig. 7. WiFED scheduling of energy and data during 802.11ac contention free period.

- It activates Point Co-ordination Function (PCF) to create a CFP that will use a brief duration of TDMA for energy transfer. Thus, there are intermittent TDMA-based PCF sessions within an existing contention-based regular DCF time duration.
- The network allocation vector (NAV) for all clients and sensors is set by the AP to the maximum expected duration of the CFP (`CFPMaxDuration` parameter).
- All frame transfers during CFP use an inter-frame spacing that is less than that of DCF-based medium access, preventing other clients/sensors from gaining access to the medium using contention based mechanisms.
- At the end of the CFP, the AP resets the NAV of all stations (including sensors) and resumes regular contention based access.

• **Starting/ending Energy Transfer Durations:** The AP announces the CFP (and upcoming energy transfer) to the network using the beacon frame. The AP terminates the CFP by transmitting a CF-End frame, which resets the NAV of all the stations (including sensors) in the BSS [16]. For those sensors scheduled for energy transfer, the AP includes the sensor's AID in the beacon frame transmitted at the start of CFP to inform the schedule of energy and data transfer slots for individual energy depleted sensors. Since the sensors wake up at the beacon intervals, they receive this information and accordingly wake up at their respective scheduled time slots for either energy or data transfer. We note that WiFED introduces delays in both PCF and DCF data traffic for STAs at the cost of supplying timely energy to the sensors. We provide quantitative results on this tradeoff later in Sec. VI.

• **Sensor Residual Energy Representation and Prediction:** In Figure 8, the residual energy representation of three sensors is depicted through data and energy time slots in CFP. The
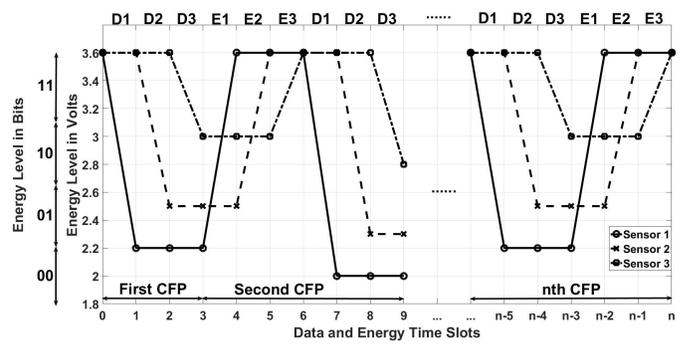

Fig. 8. Sensor residual energy graph during WiFED CFP operation of energy and data transfer.

controller divides the CFP durations into fixed data and variable energy slots for each of the three sensors. The energy slots are variable, since the controller calculates the time to charge each sensor based on their differing residual energy at the start of every CFP. Sensor 1 data and energy slots are depicted as D1 and E1, respectively, and similarly D2, E2 for Sensor 2. The energy consumption is different as each sensor is assumed to have varied application data requirements. Sensor 1 consumes most energy followed by Sensor 2 and 3, in their respective data slots. With the current bit level energy information, received from the sensors, the controller also checks if each sensor's residual energy will go below the minimum threshold for sensor operation (1.8V). If the predicted residual energy is below the threshold for a sensor, it will be added in the set of energy depleted sensors and controller schedules it for energy transfer in the next CFP. In Section V, we give detailed steps for the above calculations.

V. WiFED Energy Scheduling Framework

This section formally describes the mathematical operations performed by the controller to efficiently charge a large set of energy depleted sensors while minimizing the data communication delay. The first problem is how to identify the best subset of sensors for charging in the next CFP, without resulting in a fully energy depleted sensor. Furthermore, the formulation must also consider that other healthy sensors do not die out in the subsequent data slot, given their variable rates of data transfer for each data slot. Finally, the controller minimizes the overall charging rate for all the scheduled sensors with the limited number of ETs. The controller achieves these multiple objectives through an energy prediction scheme and global charging optimization, as described below.

A. Sensor Residual Energy Prediction

We assume the transmission power of the sensors for data transmission is fixed. Let, the sensor's transmission power for data transmission be $p^{eh}(t)$ and the start and end times for the data slot be t_{x-1} and t_x respectively. Then, energy consumed till the end of this data slot is $E_{C_{t_x}} = \int_{t_{x-1}}^{t_x} p^{eh}(t)$.

Let the transmission power of the sensor be fixed during energy charging, given as $p_f^{eh}(t)$. Then with t_{x-2} and t_{x-1} being the start and end times for energy harvesting, the energy

consumed during energy harvesting at the end of this time slot can be given as $E_{Cf_{t_{x-1}}} = \int_{t_{x-2}}^{t_{x-1}} p_f^{eh}(t)$.

If V_{max} is the maximum voltage capacity of the sensor and t_{x-2} is the end of a data slot, at which instant, the residual energy is V_{res}. Then, the required energy status at t_{x-2} for the sensor will be:

$$E_{req} = [C\frac{V_{max}^2 - V_{res}^2}{2}] \tag{2}$$

with C being the capacitor capacitance and the constraint $V_{res} \leq V_{max}$. Considering charging completes at t_{x-1}, the amount of energy that needs to be harvested in this sensor is:

$$E_{H_{t_{x-1}}} = E_{req} \tag{3}$$

with the constraint that the harvested energy $E_{H_{t_{x-1}}}$ should not exceed the maximum energy storage capacity E_{max} of the sensor:

$$E_{H_{t_{x-1}}} \leq E_{max} \tag{4}$$

Given the sensor being charged from t_{x-2} to t_{x-1} and was assigned a data slot from t_{x-1} to t_x, we formulate the residual energy at the end of time instant t_x as:

$$E_{res_{t_x}} = E_{res_{t_{x-1}}} - E_{C_{t_x}} \tag{5}$$

$$E_{res_{t_x}} = E_{H_{t_{x-1}}} - E_{Cf_{t_{x-1}}} - E_{C_{t_x}} \tag{6}$$

Substituting the values of $E_{H_{t_{x-1}}}$, $E_{Cf_{t_{x-1}}}$ and $E_{C_{t_x}}$ we get the following:

$$E_{res_{t_x}} = C\frac{V_{max}^2 - V_{res}^2}{2} - \int_{t_{x-2}}^{t_{x-1}} p_f^{eh}(t) - \int_{t_{x-1}}^{t_x} p^{eh}(t) \tag{7}$$

The controller will decide to schedule the data transmission for a sensor in the next time slot based on: (i) the status of the residual energy at the end of the current time slot, (ii) prediction of residual energy after the next data slot in this case t_{x+1}.

$$E_{res_{t_{x+1}}} = E_{res_{t_x}} - E_{C_{t_{x+1}}} \tag{8}$$

$$E_{res_{t_{x+1}}} = [C\frac{V_{max}^2 - V_{res}^2}{2}]_{t_{x-1}} - \int_{t_{x-1}}^{t_x} p^{eh}(t) - \int_{t_x}^{t_{x+1}} p^{eh}(t) \tag{9}$$

The controller checks whether this residual energy at the next time slot after data transmission is higher than the minimum threshold energy level required for all sensors, formulated as $C\frac{V_{min}^2}{2}$, where $V_{min} = 1.8 Volts$ is the minimum voltage required by all sensors to remain alive. If the predicted residual energy in the next slot, due to data transmission, is greater than the minimum energy level, given as:

$$E_{res_{t_{x+1}}} > C\frac{V_{min}^2}{2}, \tag{10}$$

then the controller schedules a time slot from t_x to t_{x+1} for that sensor's data transmission. Otherwise, the controller schedules energy harvesting for that particular sensor at a future slot. The received power at the sensor due to energy beamforming is given by (1), which is exponential to the number of ETs. Thus, from (1) and (2), the time t to fully charge a sensor can be calculated as:

$$P_T^r(t) = E_{req} \tag{11}$$

$$t_{charge} = \frac{C(V_{max}^2 - V_{res}^2)}{2P_T^r} \tag{12}$$

B. Optimization for Minimizing Charging Time

After calculating the amount of required energy and prediction of residual energy of each sensor, the controller performs the following optimization for minimizing charging time. We use K to N bipartite matching, where K ETs can be represented as a set of K nodes C_1, C_2, C_3 .. C_i .. C_K [$1 \leq i \leq K$] and N sensors by a set of N sensors as v_1, v_2, .. v_j .. v_n [$1 \leq j \leq n$]. Given a deployment of K ETs and n sensors that sent energy requests, $(n < N)$, harvested power in the 802.11ac contention free time T [$1 \leq t \leq T$] at a sensor v_j could be calculated as:

$$E_j = \eta P_j^r(t) \tag{13}$$

where η is the RF-to-DC efficiency of the energy harvesting circuit, and $P_j^r(t)$ is the received power at sensor v_j (equation 1). Accordingly, the optimization problem is to maximize the overall harvested power of the n sensors within the contention-free time reserved earlier:

$$maximize \sum_{j=1}^{n} E_j \tag{14}$$

subject to the following constraints:

$$X_{ijt} \in 0,1 \quad [1 \leq i \leq K], [1 \leq j \leq n], [1 \leq t \leq T] \tag{15}$$

$$X_{ijt} = 0 \quad if \quad [t < 1] \quad and \quad [t > T] \tag{16}$$

$$\sum_{j=1}^{n} X_{ijt} \leq 1 \tag{17}$$

$$\sum_{i=1}^{K} X_{ijt} \leq K \tag{18}$$

where (15) states that $X_{ijt} = 1$, if ET C_i is charging sensor v_j in the designated time slot t, and otherwise $X_{ijt} = 0$. Also, (16) states the sensor v_j cannot be charged outside the contention-free time period T. Additionally, (17) states that ET C_i cannot charge more than one sensor v_j in the designated time slot t and (18) indicates that sensor v_j may be charged by more than one ET in the designated time slot t. (17) and (18) indicate one ET cannot charge more than one sensor at a time, while one sensor can be charged by more than one ET at a time. Thus, we define a set of virtual nodes for each sensor to enable concurrent ET assignment to the energy requesting node. In particular, each sensor may have K virtual nodes that are designated to the available ETs. The weight of the edge connecting a virtual sensor node to one ET is represented by the harvested power contributed by the ET to the given sensor. The higher the harvested power, the weight of the link also increases, given the non-linear harvesting circuit efficiency. We solve the mapping of K ETs to N nodes by
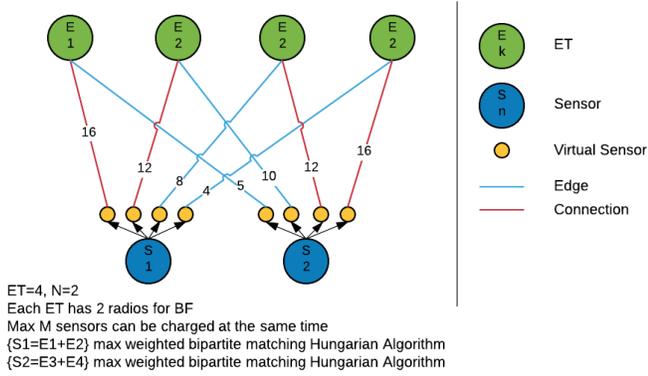
Fig. 9. Bipartite maximum weighted matching for scheduling ETs and sensors within each subgroup.

using maximum weighted matching algorithm, as shown in Figure 9. The combined weights of the edges between ETs and virtual nodes of a sensor indicate the harvested power for that sensor, and the more ETs are assigned to a sensor, the higher its harvested voltage (and the lower its charging time) become.

C. Scheduling ETs and Sensors

Our maximum weighted matching algorithm utilizes the Hungarian algorithm [17]-[18] to efficiently map the ETs with the energy depleted sensors in a given bipartite graph. We define disjoint sets $ET = \{ET_1, ET_2, ..., ET_K\}$ and $S = \{S_1, S_2, ..., S_N\}$ and form the bipartite graph, $G_{K,N}$, by taking ET and S as set of the bipartition of the vertex set of the graph. After the construction of the bipartite graph, optimal matching guarantees that each sensor gets one or more ET in a defined time slot. Algorithm 1, shows two main phases: (1) *initialization phase*, where we compute the weights based on the harvested power, and (2) *maximum weighted matching phase*.

Algorithm 1 Scheduling ETs and Sensors

1: **for** $i \leftarrow 1$ to N **do**
2:     $E_{rest_{x+1}} \leftarrow$ *compute* $\forall i \in N$
3:     **if** $E_{rest_{x+1}} < C\frac{V_{min}^2}{2}$ **then**
4:         Schedule for energy harvesting
5:         **for** $j \leftarrow 1$ to K **do**
6:             $w_{i,j} \leftarrow P_{eh}(t)$
7:         **end for**
8:     **end if**
9: **end for**
10: Sort sensors according to E_{res} in ascending order
11: Create $n = \lceil \frac{N}{\lceil K/2 \rceil - 1} \rceil$ subgroups with max $\lceil K/2 \rceil - 1$ nodes per group
12: **for** $m \leftarrow 1$ to n **do**
13:     $i = (m - 1) \times (\lceil K/2 \rceil - 1) + 1$
14:     $j = m \times (\lceil K/2 \rceil - 1)$
15:     Constitute KxK complete bipartite graph based on K ETs and virtual nodes associated from n_i to n_j
16:     Best Matching(m) $\leftarrow$ use Hungarian algorithm to get the maximum weighted matching
17: **end for**
18: **return** Best Matching

At 802.11ac NDP duration, let N sensors demand energy from K ETs. The controller sorts the sensors in ascending order of their residual energy level. Then, it divides N sensors into n subgroups $[n_1, n_2, .. n_i, .. n_n]$ such that the maximum number of sensors in each group is allocated as $\lceil K/2 \rceil - 1$ and total number of subgroups would be $\lceil \frac{N}{\lceil K/2 \rceil - 1} \rceil$. This guarantees each sensor will be assigned two and more ETs for distributed beamforming. Figure 9 depicts the corresponding constructed graph for each subgroup, where an edge represents all possible relations from a given sensor to ETs and the line connection represents the assignments between ETs and sensor pairs based on their weights. The sensors in subsets $[n_1, n_2, .. n_i, .. n_n]$ are in ascending order of residual energy level, i.e., the sensors in n_1 have the least residual energy while the sensors in n_n have the highest residual energy. Additionally, sensors are assigned charging time slots in ascending order of the residual energy. n_1 is assigned the first slot while n_n is assigned the last slot. The matching algorithm picks the best ETs to charge each sensor in the group n_i at the i_{th} time slot.

After this selection, the duration of the i_{th} slot is calculated based on the maximum time to finish the simultaneous charging of all the sensors in the group n_i. Similar mapping and calculation for charging time is completed for the remaining n_{n-i} groups. In this way, the controller calculates the time duration for each slot and the overall required charging time for N sensors. The data slots for the 802.11ac users will be allocated in the CFP time after the charging the sensors.

VI. PERFORMANCE EVALUATION

In this section, we extensively evaluate data and energy performance metrics of the WiFED. We have implemented our system through integration of a distributed energy transfer module with NS-3. First, we evaluate system wireless energy transfer performance in terms of charging time, and then we investigate the system data performance in terms of packet error rate, average throughput, and latency by comparing with three schemes: 802.11ac with random energy transmission, 802.11ac with continuous data transmission, and 802.11ac without energy transfer.

A. Simulation Setup

We consider variable number of sensors that are randomly deployed in 20x20 m^2 area with multiple ETs and in a space with an active 802.11ac AP connected to a controller. We ran the simulation 300 times at each instance of number of sensors, ETs, packet size and packet numbers. Before each evaluation, the batteries on each sensor are set to a maximum voltage level, V_{max}=3.65 Volts. The characteristics of the sensor, such as power of transmission, reception, sensing, sleeping, channel bandwidth are set based on micro-controller TI MSP430F2274, and 2.4 GHz CC2500 radio chip. The capacitance of the capacitor, C, is $5700\mu F$, and all ETs have the same transmission power as P_t=3 Watts. Transmitter and receiver antenna gain are set to G_t=3.98 dBi, and G_r=1 dBi.

B. Energy Performance Analysis

As the baseline energy performance comparison, Figure 10(a) shows a distance-based matching scenario where the controller groups the sensors according to the position of ETs.
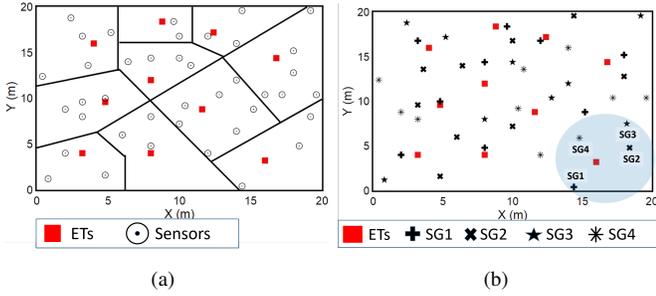
(a)

(b)

Fig. 10. Two scenarios of network topology: N=40, K=10 (a) Closest distance assignment (b) WiFED assignment into subgroups based on residual energy.
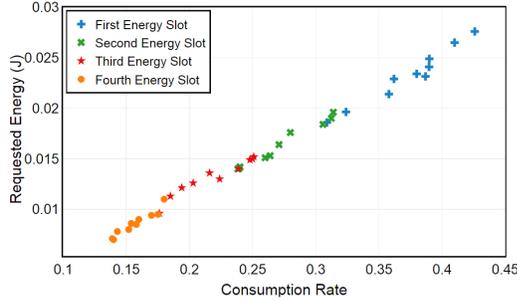

Fig. 11. Requested energy level (J) w.r.t. consumption rate for 40 sensors at a time interval.
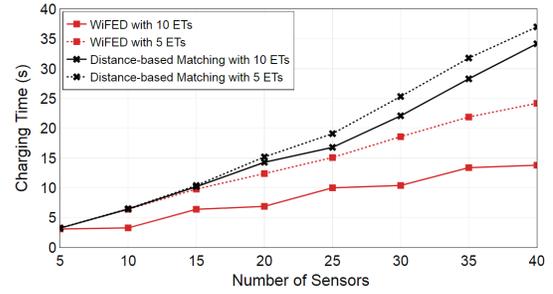

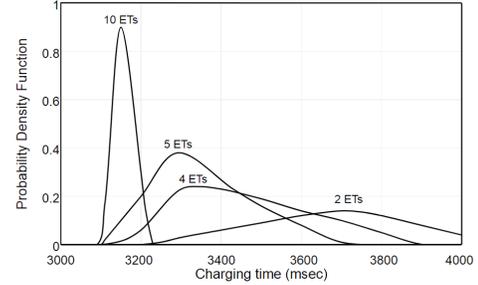
Fig. 12. Charging time (s) w.r.t number of sensors.

Fig. 13. Probability density function of charging time (msec) for one node. The number of ETs is defined as 10, 5, 4 and 2. The number of sensors is equal to 5.

Figure 10(b) presents the WiFED scenario where the sensors are scheduled into optimal subgroups (SGs) via our bipartite matching algorithm from Sec. V-C. First, we set the number of ETs at 10 and the number of sensors at 40, and measure the required energy level of each sensor according to residual energy level with equation (2), shown in Figure 11. We calculate the ratio of consumed energy at a given time instant and accordingly show the scheduling of sensors to be served in subsequent energy slots. We see that almost all the nodes with high energy consumption rates are scheduled for energy harvesting in the first slot. Additionally, residual energy and consumption rates are not unique and independently impact the energy harvesting in a time slot.

Figure 12 shows the average charging time with deployment of 5 and 10 ETs. We see that WiFED provides significant improvement in terms of charging time compared to the distance based scenario. Synchronizing transmit and receive times at sensors and scheduling the ETs over sensors have enabled 15% improvement in network lifetime due to less time to charge. In distance-based matching scenario, we observe that when sensors are deployed in higher density, more sensors go out of service as each ET can only serve a limited number of sensors within its range and cannot predict the priority of sensors and each ET randomly transfers power to the sensors within its operation area. A sensor node that is far away from the ET will have a lower energy harvesting level than a sensor node that is close to the ET. In this case, energy levels of sensors are not taken into account and there is no mechanism to gather information such as requested energy, residual energy, and consumed energy.

We next investigate how charging time changes based on the number of ETs. Figure 13 shows the probability density function of charging time for one sensor. Here, we set the

number of sensors to 5. As seen in the Figure 13, when the number of ETs increases to 10, the probability of each sensor getting charged by more than one ET at a time will increase and this will result in a lower charging delay. On the other hand, when the number of sensors is higher than the number of ETs, such as 2 ETs, the controller groups the sensors based on the residual energy and data transmission, and then schedules the sensors. Compared to distance-based matching, WiFED contributes 31% reduction in the charging delay.

C. Data Performance Analysis

For calculating the data performance, we simulate four scenarios with varying number of sensors and ETs: (i) WiFED, (ii) 802.11ac with Random Energy Transmission (RET), (iii) 802.11ac with Continuous Energy Transmission (CET), and (iv) 802.11ac without energy transmission. We compare the results as seen in Figure 14 in terms of latency, packet error rate and throughput.

To measure latency, the packet generation rate is set to 10 packets per second, with packet size of 100KB. As shown in Figure 14(a), WiFED experiences much less latency, compared to 802.11ac with RET and CET, because WiFED manages the energy transfer process to co-exist with WiFi. We calculate PER and throughput in the four scenarios given in Figures 14(b)-14(c). To measure PER, the number of packets correctly received are observed along with their respective signal strengths. The average throughput per node is calculated for varying number of sensors. We observe a significant improvement in WiFED throughput and PER, due to the co-existence support. On the other hand, with 802.11ac RET and CET, the probability of data signals being interrupted greatly increases, resulting in higher packet error rate and reduced throughput. Interestingly, Figure 14(c) shows the throughput of the network is better in WiFED than in the scenario with
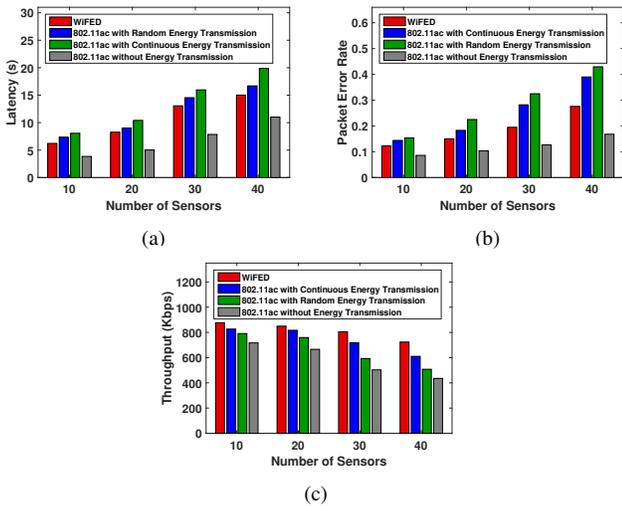
Fig. 14. (a) Latency (b) Packet error rate (c) Throughput w.r.t. varying number of sensor.
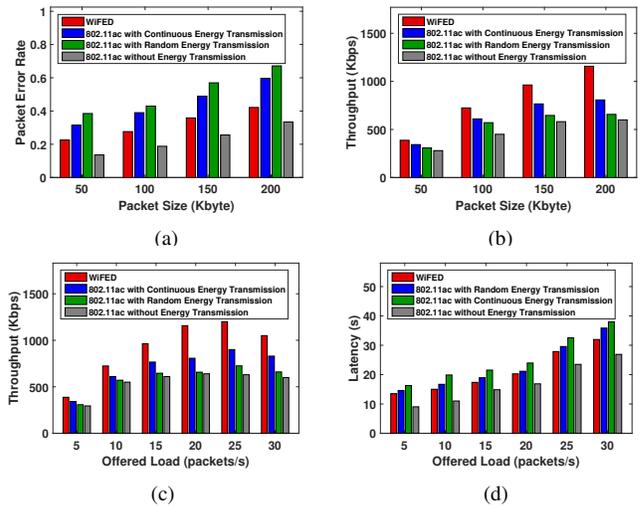

Fig. 15. (a) Packet error rate and (b) Throughput w.r.t. packet size when offered load is equal to 10 packets/s (c) Throughput and (d) Latency w.r.t. offered load (packet/s) when packet size is equal to 100Kbytes.

no energy transfer. Also, RET and CET scenarios perform better than in the case of no energy transfer. This is because in RET and CET, because of no scheduling, some sensors get completely depleted of energy and stop transmitting data, whereas those sensors in the region of energy reception cannot transmit data because of interference. This creates *holes* in the network topology that decreases the number of competing users for channel access. Also, the WiFED controller co-ordinates data and energy transfer in a time scheduled manner, which negates the eliminates such *holes* and interfering signals. From Figure 15, we see the results of data transmission in our four scenarios with varying number of packet size and offered load (packets/s). We conducted the simulation with 10 ETs and 40 sensors. These results show that both 802.11ac RET and CET will adversely affect the performance of data and energy transmission. Thus, WiFED provides better results in terms of throughput and packet error rate while 802.11ac with RET and CET offers no improvement in data transmission.

VII. CONCLUSION

We have devised a data and energy co-existence approach using in-band 802.11ac protocol defined features for distributed energy beamforming through dedicated transmitters. We have demonstrated the feasibility of a practical system with preliminary experiments and extensive simulations. Comparing the performance of data and energy delivery in WiFED with constant and random energy transfers, we see that our approach enables seamless co-existence within the legacy WiFi protocols, while achieving 31% reduction in charging delay and 15% improvement in sensor lifetime.

VIII. ACKNOWLEDGMENT

REFERENCES

[1] P. Rawat, K. D. Singh, H. Chaouchi, and J. M. Bonnin, "Wireless sensor networks: a survey on recent developments and potential synergies", the Journal of supercomputing, 68(1), 1-48.

[2] FCC Rules, https://www.fcc.gov/general/rules-regulations-title-47

[3] E. Zhi Ang, H. Tan, and W. KG Seah, "Design and performance analysis of MAC schemes for wireless sensor networks powered by ambient energy harvesting", Ad Hoc Networks, vol. 9, no. 3, pp. 300-323, 2011.

[4] F. Xenofon, and N. Dragoni, "ODMAC: an on-demand MAC protocol for energy harvesting-wireless sensor networks", ACM MSWiM 2011.

[5] R. G. Cid-Fuentes, M. Y.Naderi, S. Basagni, K. R. Chowdhury, A. Cabellos-Aparicio, and E. Alarcn, "On signaling power: communications over wireless energy", IEEE INFOCOM 2016.

[6] L. Xiao, P. Wang, D. Niyato, D. I. Kim, and Z. Han, "Wireless networks with RF energy harvesting: a contemporary survey", IEEE Communications Surveys & Tutorials 17, no.2, pp. 757-789, 2015.

[7] X. Lu, P. Wang, D. Niyato, D. I. Kim, and Z. Han, "Wireless charging technologies: fundamentals, standards, and network applications", IEEE Communications Surveys and Tutorials, vol. 18, pp. 1413-1452, 2016.

[8] S. Lee, R. Zhang, and K. Huang, "Opportunistic wireless energy harvesting in cognitive radio networks", IEEE TWC, vol. 12, no. 9, pp. 4788-4799, Sep. 2013.

[9] A. A. Nasir, X. Zhou, S. Durrani, and R. A. Kennedy, "Relaying protocols for wireless energy harvesting and information processing", IEEE TWC, vol. 12, no. 7, pp. 3622-3636, July 2013.

[10] W. Xu, W. Liang, S. Hu, X. Lin, and J. Peng, "Charging your smartphones on public commuters via wireless energy transfer", IEEE IPCCC 2015.

[11] M. Y. Naderi, K. R. Chowdhury, and S. Basagni, "Wireless sensor networks with RF energy harvesting: energy models and analysis", IEEE WCNC 2015.

[12] R. Mudumbai, J. Hespanha, U. Madhow, and G. Barriac, "Distributed transmit beamforming using feedback control", IEEE Transactions on Information Theory, vol. 56, no. 1, pp. 411-426, Jan. 2010.

[13] R. Palacios-Trujillo, J. Alonso-Zarate, N. L. da Fonseca, and F. Granelli, "Maximum achievable energy efficiency of TXOP power save mode in IEEE 802.11 ac WLANs", IEEE GLOBECOM 2016.

[14] G. Matthew, "802.11 ac: a survival guide: Wi-Fi at gigabit and beyond", O'Reilly Media Inc., 2013.

[15] Wireless LAN medium access control (MAC) and physical layer (PHY) specifications–amendment 4: enhancements for very high throughput for operation in bands below 6 GHz., "IEEE std 802.11ac-2013", pp.1-425, Dec. 2013.

[16] E. Perahia, and R. Stacey, "Next generation wireless LANs: 802.11n and 802.11ac", Cambridge: Cambridge University Press, 2013.

[17] H. W. Kuhn, "The hungarian method for the assignment problem", Naval Research Logistics Quarterly 2, pp. 83-97, 1955.

[18] J. Munkres, "Algorithms for the assignment and transportation problems", Journal of the Society for Industrial and Applied Mathematics vol. 5, no. 1 pp. 32-38, 1957.